



HAL
open science

Physical-statistical and wideband model of the land mobile satellite propagation channel

Israel Jonathan

► **To cite this version:**

Israel Jonathan. Physical-statistical and wideband model of the land mobile satellite propagation channel. IEEE-APS Topical conference on Antennas and propagation in Wireless Communications (APWC 2022), Sep 2022, Le Cap, South Africa. 10.1109/APWC49427.2022.9899923 . hal-03878404

HAL Id: hal-03878404

<https://hal.science/hal-03878404>

Submitted on 29 Nov 2022

HAL is a multi-disciplinary open access archive for the deposit and dissemination of scientific research documents, whether they are published or not. The documents may come from teaching and research institutions in France or abroad, or from public or private research centers.

L'archive ouverte pluridisciplinaire **HAL**, est destinée au dépôt et à la diffusion de documents scientifiques de niveau recherche, publiés ou non, émanant des établissements d'enseignement et de recherche français ou étrangers, des laboratoires publics ou privés.

Physical-statistical and wideband model of the land mobile satellite propagation channel

ISRAEL Jonathan

ONERA/DEMR, Université de Toulouse Toulouse, France

jonathan.israel@onera.fr

Abstract—This paper presents an extension of the SCHUN (Simplified CHannel for Urban Navigation, [1]) simulator and its validation framework in a wideband context. The hybrid physical-statistical model on which this simulator relies on extends the scope of applicability of standard channel characterization models thanks to its physical modeling of the interactions between the environment and a receiver. It also allows the generation of frequency and polarization diversities, and it improves the representativeness of the urban environment (type of materials, roughness...) while keeping a reasonable computational payload. This model has been validated in a narrowband and wideband context with respect to data acquired in a LMS (Land Mobile Satellite) configuration.

Index Terms—Land Mobile Satellite Propagation Channel, Physical-statistical model

I. INTRODUCTION

The physical interactions between an incident electromagnetic wave and the environment close to a mobile receiver in an urban environment have a primordial effect on the characteristics of the received signal and therefore on the performance of the associated systems, especially in the field of satellite communications and GNSS (Global Navigation Satellite System). The modeling of these interactions is thus necessary for the simulation of the performances of such systems in a constrained environment. Three main families of methods are used to represent these interactions: deterministic, physical-statistical and statistical. Deterministic approaches are based on a realistic modeling of the 3D environment and its electromagnetic properties (roughness, dielectric parameters...) and on a deterministic calculation (exact or approximate) of the interactions to simulate the received signal. Such simulators, based for instance on asymptotic methods like [2], [3], [4], [5], allow to obtain accurate results but often require a good knowledge of the environment and an important computation time depending on the complexity of the environment and the frequency of the emitted wave. On the other hand, statistical approaches use mainly existing data and little or no physics to simulate the received signal, often from regression of parametric models on measured databases. This is the case for example for the propagation model provided in the ITU-R (International Telecommunication Union - Recommendation) P681 in its paragraph 6, [6]. A two-state, narrowband Markov model is regressed on S and C band data and the resulting parameters are used to simulate narrowband time series. This type of approaches offers the advantage of a reduced computational payload and ensures by construction

the correspondence between the statistics of simulated signals and the measurements, at least at the frequency and in the type of environment where the regression has been performed. On the other hand, since it introduces little or no physics into the modeling, no applicability of such methods when changing frequency or type of environment can be guaranteed. Between these two domains, hybrid or physico-statistical methods often allow to achieve a compromise in representativeness of the scene and the physical rendering and simplicity in terms of scene modeling and computational cost. The model of paragraph 7 of the ITU-R P681 recommendation falls into this category although the physical parameters introduced in the modeling of scatterers are essentially based on regressions and not on physical modeling. The SCHUN simulator used in this study, [1], is based on a simplified representation of the urban environment allowing an approximate but physical calculation of the electromagnetic interactions.

II. PRESENTATION OF THE PHYSICAL-STATISTICAL MODEL

A. Generic overview

The simulation of electromagnetic scattering from buildings is based on the EM (Electro-Magnetic) SCHUN simulator initially developed for GNSS simulations in urban areas. The fundamental principles governing the SCHUN simulator are perfectly extensible to a model applied in another frequency band (especially between X and Ka). The concept of the SCHUN EM interaction simulator is to generate the environment using a virtual city approach and model the interactions using simplified EM models. This trade-off allows for fast computations relying on physical models.

The macro architecture of the SCHUN channel simulator is shown in Fig.1. The statistical component of this approach is represented by the virtual city generation. All other modeling elements are based on ray techniques and physical EM models. The simplified building interaction models are based on physical EM models of models such as GO (Geometric Optics) and PO (Physical Optics). The direct signal shadowing model is based on UTD (Uniform Theory of Diffraction). The SCHUN channel simulator is capable of providing a wide range of results such as CIRs (Channel Impulse Responses) in delay/Doppler space, DoA (Directions of Arrival) information, complex narrowband signals, power time series, Doppler spectrums or masking time series.

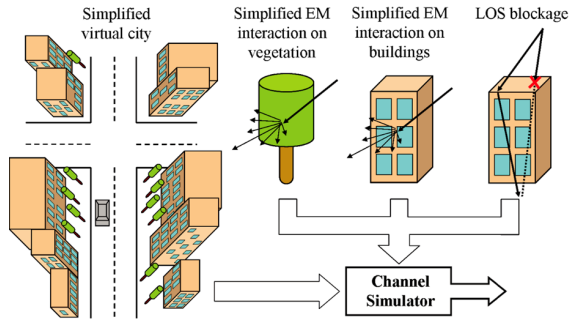


Fig. 1. Macro architecture of the SCHUN LMS channel simulator.

B. Approach of the Three Component Model (3CM)

The SCHUN building scattering model is based on EM models with a minimum use of empirical approaches or measurement campaigns and satisfy the trade-off between computation time and versatility.

The scattering phenomenon taking place around complex façades can be divided into three propagation mechanisms, or components, each one being linked to a particular propagation scheme. The three components on which relies the 3CM are presented in Fig.2. This scattering decomposition principle has the advantage of being potentially applicable to existent ray-tracing tools without major modifications.

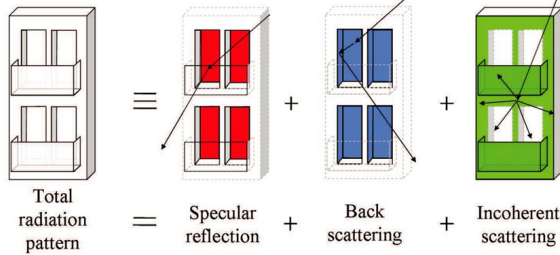


Fig. 2. Decomposition principle of the 3CM.

The 3CM model relies on the three propagation components:

- The specular component: it reproduces the forward reflection mechanism taking place on wide and smooth surfaces such as windows and flat walls. This component is the most powerful. In its implementation, the specular component is based on a simplified version of the PO algorithm.
- The backscattering component: it reproduces a double bounce reflection, or backward reflection, due to dihedral effects taking place near protruding and receding elements of the façade, i.e. receding windows or protruding balconies. The backscattering component is less powerful than the specular one but is responsible of significant contributions coming from the opposite side of the LOS signal. From existent models, this component is usually integrated into the incoherent scattering mechanism al-

though the EM mechanism is coherent and different. The implementation of the backscattering component is also based on a simplified version of the PO algorithm.

- The incoherent scattering component: it reproduces the scattering phenomenon coming from all small features present on complex façades. This component allows a smoother transition between the specular zone and the backscattering zone. It also characterizes the influence zone of the façade. Since small features are not supposed to be modelled using asymptotic methods such as PO, the implementation of this empirical component is based on analytical models extracted from [7].

The main advantage of the approach chosen for the 3CM is the reduced computational payload: the total scattering pattern of any complex façade can be divided into three components, each one being easy to model. Another advantage of the 3CM is its physical EM base which leads to realism and versatility. Contrary to empirical models, the 3CM is able to generate wideband CIRs with realistic delay, Doppler and DoA information. Since it is based on the PO algorithm, the 3CM can also deal with dielectric materials, handle elliptic polarizations and is scalable in frequency from 1 to 5GHz. Finally, the 3CM is suitable for MIMO studies with transmitting/receiving diversity, polarization diversity or frequency diversity.

C. Modelling of the trees and poles

The tree scattering model is based on the multiple scattering theory, [8]. It separates the effects due to the trunk and to the tree canopy. The trunk is modelled by a cylinder which allows taking into account the blocking and the diffraction effect on the edges of the cylinder. When going through the canopy, the incoming wave will be attenuated (the linear specific attenuation being fixed for a given type of tree) and a multipath diffuse component is also computed. This latter effect is based on the random positioning of point scatterers in the canopy which will diffuse in all directions. The pole interaction model is also a diffraction model based on UTD.

III. VALIDATION FRAMEWORK

A. Experimental data

On the transmitter side, the experimental setup consists of a high phase stability frequency generator (Agilent E8267D PSG) and a 15W RF amplifier. The PROMOLAB recorder is mounted on a trailer towed by a passenger car. The two antennas for each band are wired simultaneously on the roof of the trailer. The core of the post-processing algorithm is based on the correlation between a known reference PRN (Pseudo-Random Noise) code in the data samples and the locally generated code following a method similar to GNSS signal processing. This method was chosen because, like the GNSS signal, the received signal power is below the noise floor of the digitization chain.

At the receiving chain, the locally generated PRN code is used to perform the acquisition process by estimating the correlation peak. In addition, the various correlation peaks allow multipath to be highlighted and thus provide a broadband

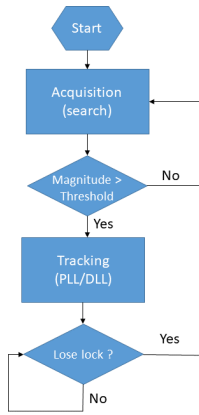


Fig. 3. State machine of the processing chain allowing the acquisition and tracking of the transmitted signal.

characterization of the signal. When the amplitude of the main correlation peak is sufficient, the acquisition is successful and a rough estimate of the signal delay and Doppler is made. In the opposite case, for example when the receiver is behind a building or a tree with a dense canopy, a new acquisition is performed until becoming successful. Then, the processing loop enters the tracking phase where the delays and Doppler shifts of the code are estimated in order to lock the processing chain to the direct path. When the tracking fails to follow the direct path, the processing loop re-enters the acquisition stage until being successful. This general scheme is shown in Fig. 3.

B. Validation of the simulation model

The reconstructed street has been used as input in the SCHUN simulator in order to perform a site specific comparison between the simulation and the measurements in S Band on this 380 m trajectory, Fig.4.



Fig. 4. Saint-Lary main street used for measurements and simulation comparison.

The corresponding narrowband time series are shown on Fig.5. Both time series exhibit strong similitude: the main shadowing parts are located at similar locations in both cases

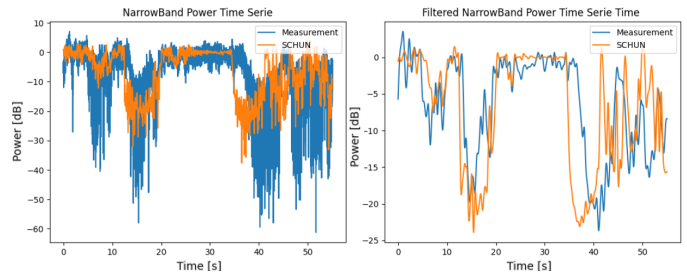


Fig. 5. Comparison of measured and simulated original (left) and filtered (right) narrowband time.

and correspond to the same order of magnitude of fading amplitude. This similitude is clearly visible on all narrowband characteristic parameters, Fig. 6. The fading amplitudes and average durations are very close to each other. The order of magnitude of the level crossing rate is also similar even though it is a little bit higher in the measurements. This characteristic has already been noticed during the SCHUN development process, [1]. This is due to the fact that in the shadowing areas, SCHUN models a vast but still limited number of electromagnetic contributors, leading to a global contribution that does not exhibit as much constructive and destructive interactions as in the reality. Therefore, the SCHUN signal is more continuous with less second order component than the measured signal. Finally, the Ricean factors are also similar in the simulation and the measurements, the main differences appearing for positive values corresponding mostly to LOS (Line Of Sight) situations: the signal is flatter in LOS situation in the simulation than in the measurement, where noise remains due to calibration and tracking residual errors.

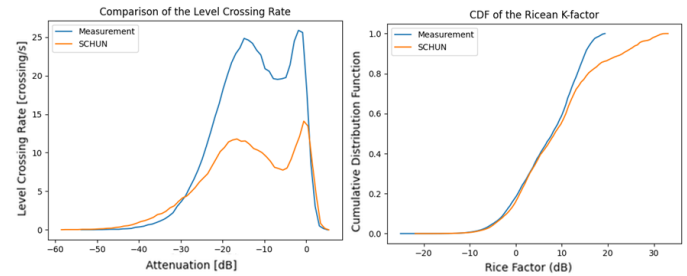


Fig. 6. Comparison of measured and simulated level crossing rates (left) and Ricean factors (right).

C. Wideband parameters

At the end of the signal processing stage, range/time maps are directly available and can be compared to the range/time maps obtained by the SCHUN simulation. In order to be comparable, the raw SCHUN range time maps have been convoluted by a triangle reproducing the signal correlation process as obtained by the GNSS-like signal processing stage applied to the measured data. The corresponding range/time maps are given in Fig. 7. Once again appear phenomena already detected in the narrowband comparison, such as the

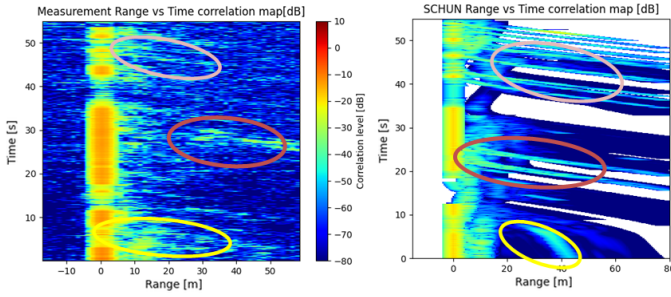


Fig. 7. Comparison of measured (left) and simulated (right) range/time maps.

blocking or fading processes visible around $t = 15$ s or $t = 40$ s for instance. Furthermore, some multipaths can also be seen on both maps, even if they may not be located exactly at the same locations, which is due to the complexity of reproducing exactly (up to a 1m and a 1s resolution) the scene and trajectory characteristics. They are shown in ellipses in both figures, the red one corresponding to multipaths due to the façade shown in Fig.8. Globally, two main differences can be noticed: while the range/time map in the measurement is dense (each pixel corresponding to a given value of the GNSS correlation process), the range/time map in the SCHUN simulation is sparse since SCHUN does not compute a dense but a discrete number of contributors which may not fill the entire map. Furthermore, the scattering life time of contributors may be larger in some cases (e.g. the pink section) due to simplifications made in the inter-objects masking computation.

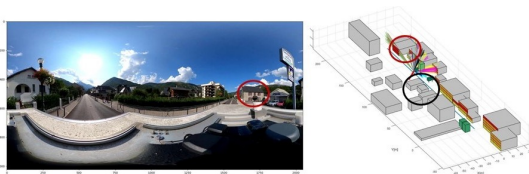


Fig. 8. Example of multipaths created by the side of a building.

From the measured and simulated range/time maps, the mean power range profiles along the trajectory are computed and given in Fig. 9.

Their shapes are close to each other although the measurement curve is more continuous than the simulated one that exhibits a discontinuity around 4 meters due to the fact that in the simulation environment, no multipath occurs with shorter delays since we did not introduce closer objects like other vehicles.

In Fig.10 are shown the spectrograms obtained from the measurement and the simulation. The main shape is the same, balancing toward the positive Doppler shifts due to the geometric configuration and leading to Doppler frequencies up to 100 Hz in both cases.

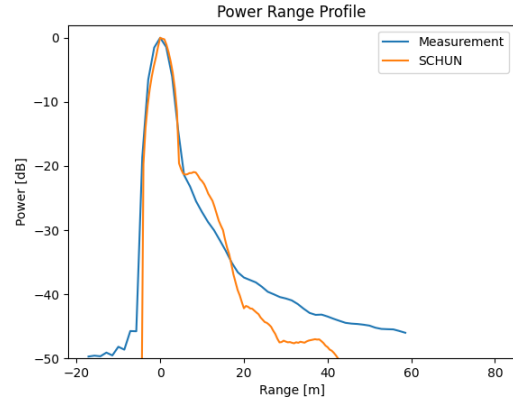


Fig. 9. Comparison of measured and simulated power range profiles.

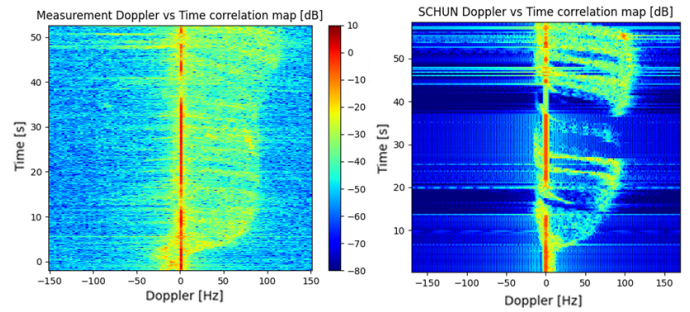


Fig. 10. Comparison of measured (left) and simulated (right) spectrograms.

IV. CONCLUSION

A validation of the SCHUN LMS model in S band is presented here. Based on GNSS signal processing techniques, the channel sounding methodology allows to retrieve wideband parameters of the propagation channel and to compare them to SCHUN simulations in either site specific (requiring the precise reconstruction of a given street) and site generic (using a virtual city generation) situations. Globally, a good correspondence has been obtained between simulations and measurements for narrowband and wideband parameters. Some limitations have been pointed out in the SCHUN simulator, either on physical or informatics levels. It leads to potential future improvements that could allow the use of this simulator in multi-frequency and multi-polarization simulations in all kinds of urban environments.

ACKNOWLEDGMENT

This work has been financially supported by CNES study DSO/RF/ITP2017.0011547.

REFERENCES

- [1] M. Ait-Ighil, J. Lemorton, F. Perez-Fontan, F. Lacoste, P. Thevenon, C. Bourga, and M. Bousquet, "Schun - a hybrid land mobile satellite channel simulator enhanced for multipath modelling applied to satellite navigation systems," in *2013 7th European Conference on Antennas and Propagation (EuCAP)*, 2013, pp. 692–696.

- [2] J. Israel, G. Carrie, and M. Ighil, "A wideband and multifrequency propagation channel simulation," in *Antennas and Propagation (EuCAP), 2013 7th European Conference on*, April 2013, pp. 677–680.
- [3] H. Mametsa, A. Berges, and N. Douchin, "Improving RCS and ISAR image prediction of terrestrial targets using random surface texture," in *Radar Conference - Surveillance for a Safer World, 2009. RADAR. International*, Oct. 2009, pp. 1 –5.
- [4] H. Mametsa, S. Laybros, A. Berges, P. Combes, P. N'Guyen, and P. Pitot, "FERMAT: a high frequency em scattering code from complex scenes including objects and environment," in *First European Conference on Antennas and Propagation, 2006. EuCAP 2006*, Nov. 2006, pp. 1 –4.
- [5] J. Israel, F. Lacoste, H. J. Mametsa, and F. P. Fontan, "A propagation model for trees based on multiple scattering theory," in *Antennas and Propagation (EuCAP), 2014 8th European Conference on*, April 2014, pp. 1255–1258.
- [6] "ITU-R P681-11, propagation data required for the design systems in the land mobile-satellite service." [Online]. Available: <https://www.itu.int/rec/R-REC-P.681-11-201908-I/fr>
- [7] G. Ruck, D. Barrick, W. Stuart, and C. Krichbaum. Plenum Press, 1970.
- [8] J. Israel and A. Pajot, "Fading and scattering due to trees in l to ka band propagation simulations," in *2015 9th European Conference on Antennas and Propagation (EuCAP)*, 2015, pp. 1–5.